applied sciences

MDPI

Communication

Glycerol Flow through a Shielded Coil Induces Aggregation and Activity Enhancement of Horseradish Peroxidase

Yuri D. Ivanov [1,2,*], Ivan D. Shumov [1], Andrey F. Kozlov [1], Maria O. Ershova [1], Anastasia A. Valueva [1], Irina A. Ivanova [1], Vadim Y. Tatur [3], Andrei A. Lukyanitsa [3,4], Nina D. Ivanova [3,5] and Vadim S. Ziborov [1,2]

[1] Institute of Biomedical Chemistry, Pogodinskaya Str., 10 Build. 8, 119121 Moscow, Russia; shum230988@mail.ru (I.D.S.); afkozlow@mail.ru (A.F.K.); motya00121997@mail.ru (M.O.E.); varuevavarueva@gmail.com (A.A.V.); i.a.ivanova@bk.ru (I.A.I.); ziborov.vs@yandex.ru (V.S.Z.)
[2] Joint Institute for High Temperatures of the Russian Academy of Sciences, 125412 Moscow, Russia
[3] Foundation of Perspective Technologies and Novations, 115682 Moscow, Russia; v_tatur@mail.ru (V.Y.T.); andrei_luk@mail.ru (A.A.L.); ninaivan1972@gmail.com (N.D.I.)
[4] Faculty of Computational Mathematics and Cybernetics, Moscow State University, 119991 Moscow, Russia
[5] Moscow State Academy of Veterinary Medicine and Biotechnology Named after Skryabin, 109472 Moscow, Russia
* Correspondence: yurii.ivanov.nata@gmail.com

Abstract: Glycerol has found its applications as a heat-transfer fluid in heat exchangers, and as a component of functional liquids in biosensor analysis. Flowing non-aqueous fluids are known to be able to induce electromagnetic fields due to the triboelectric effect. These triboelectrically generated electromagnetic fields can affect biological macromolecules. Horseradish peroxidase (HRP) is widely employed as a convenient model object for studying how external electric, magnetic, and electromagnetic fields affect enzymes. Herein, we have studied whether the flow of glycerol in a ground-shielded cylindrical coil affects the HRP enzyme incubated at a 2 cm distance near the coil's side. Atomic force microscopy (AFM) has been employed in order to study the effect of glycerol flow on HRP at the nanoscale. An increased aggregation of HRP on mica has been observed after the incubation of the enzyme near the coil. Moreover, the enzymatic activity of HRP has also been affected. The results reported that their application can be found in biotechnology, food technology and life sciences applications, considering the development of triboelectric generators, enzyme-based biosensors and bioreactors with surface-immobilized enzymes. Our work can also be of interest for scientists studying triboelectric phenomena, representing one more step toward understanding the mechanism of the indirect action of the flow of a dielectric liquid on biological macromolecules.

Keywords: horseradish peroxidase; glycerol; enzyme aggregation; enzymatic activity; liquid flow

Citation: Ivanov, Y.D.; Shumov, I.D.; Kozlov, A.F.; Ershova, M.O.; Valueva, A.A.; Ivanova, I.A.; Tatur, V.Y.; Lukyanitsa, A.A.; Ivanova, N.D.; Ziborov, V.S. Glycerol Flow through a Shielded Coil Induces Aggregation and Activity Enhancement of Horseradish Peroxidase. *Appl. Sci.* **2023**, *13*, 7516. https://doi.org/10.3390/app13137516

Academic Editors: Christos Tsamis and Danijela Randjelović

Received: 19 April 2023
Revised: 23 June 2023
Accepted: 23 June 2023
Published: 26 June 2023

1. Introduction

Glycerol, a trihydric alcohol, is employed as a heat transfer fluid [1], representing a non-toxic alternative to widely used ethylene glycol [2]. Furthermore, glycerol finds its application in flow-based biosensors as a component of specialized buffer solutions [3]. The abovementioned applications can be used for the organization of a fluid flow.

Regarding biosensor systems, biological macromolecules under study are either introduced directly into the flow or immobilized on the sensor surface, which is in direct physical contact with the fluid flow [3–7]. In this situation, the fluid flow is directly interacting with the biological macromolecules. Regarding bovine serum albumin (BSA), Dobson et al. demonstrated that the direct action of a fluid flow on biological macromolecules can induce their aggregation [8]. It should be emphasized that the fluid flow can also act on biological macromolecules indirectly. In other words, the fluid flow can affect biological macromolecules even when there is no direct mechanical contact between the molecules

and the flow. Below, we consider one of the possible mechanisms of the indirect action of the fluid flow on enzymes.

The flow of both aqueous [9–15] and non-aqueous [16–21] fluids can well cause the triboelectric generation of electric charge [9–21]. This widely employed phenomenon is the development of the so-called triboelectric generators [11–14,18]. It should be emphasized that, despite the fact that aqueous fluids are used for this purpose, in the majority of cases [11–14], the successful development of oil-employing triboelectric devices was recently reported [18]. Yoo et al. have found that, in the case of glycerol, the triboelectric generation of charge is very significant in comparison with the majority of other liquids tested [21]. In this context, it should be borne in mind that triboelectrically induced fields can influence biological macromolecules [15–17], exhibiting an indirect action of a fluid flow on these macromolecules. Additional attention should also be paid in the case of the triboelectric effect of fluid flow through pipes [9,21], including pipe coils, which are used as heat exchangers in bioreactors [22]. Heat exchangers are key components of bioreactors operating with enzymes [23,24]. Since glycerol, which was found to be triboelectrically active [21], is often used as a heat transfer agent [1], further research is required in order to investigate the possible effects of its flow on biological molecules, including enzymes. And this is the aim of our study.

The effect of an external triboelectrically induced field on biological macromolecules is often manifested in the form of the aggregation of these macromolecules under the field action [15–17]. Atomic force microscopy (AFM) represents a powerful method, which allows one to investigate the aggregation of biological macromolecules [25–27], including enzymes [15–17,28–34] with high (up to single-molecule) resolution. This feature of AFM allows one to even reveal subtle effects, which are indistinguishable by macroscopic methods such as spectrophotometry [29].

AFM is widely employed for studying the aggregation state of various enzymes. In [31], AFM has allowed to determine the ratio between monomers and oligomers of cytochrome CYP102A1, whose oligomers were reported to have a higher enzymatic activity than its monomers [35]. Namely, with the use of an AFM probe with typical (10 nm) tip curvature radius, this ratio was found to be 0.5:0.5. Moreover, the use of a supersharp AFM probe with tip curvature radius of 2 nm has allowed the determination of the ratio between different oligomers of this enzyme (dimers/trimers/tetramers = 0.3:0.1:0.1). This example clearly illustrates the excellent suitability of AFM for enzyme aggregation studies. Furthermore, Baron et al. [32] discussed the influence of isopropanol on enzyme–enzyme and enzyme–surface interactions on the adsorption of lipase (isolated from *Bacillus megaterium* CCOC P2637) on polypropylene and silicon substrates. These authors have demonstrated that the addition of isopropanol to a buffered aqueous solution of the lipase promotes its disaggregation, forcing its adsorption onto hydrophilic surfaces. With the example of glutamate dehydrogenase, Blasi et al. [33] and Zhang and Tan [34] demonstrated the applications of AFM for the characterization of enzyme-functionalized surfaces.

Horseradish peroxidase (HRP) represents a ~44 kDa [36] enzyme glycoprotein, whose structure is stabilized by carbohydrate chains [37,38]. Since this enzyme is comprehensively characterized in the literature [39], many authors have used it as a model object for studying the effect of electric [40], magnetic [41–44] and electromagnetic [15–17,45–48] fields on enzymes. Previously, we reported the successful use of AFM for the revelation of HRP aggregation under the influence of flow-induced electromagnetic fields [15–17]. Sun et al. [43,44] employed AFM for the investigation of the influence of alternating magnetic fields on HRP adsorption onto mica, and revealed that the action of the field on the enzyme forces it to form complex extended structures on the substrate surface. Wasak et al. [41] studied the effect of low-frequency rotating magnetic fields on HRP. These authors have found an increase in the enzymatic activity of HRP against o-dianisidine at 1 Hz and 20 Hz magnetic field frequencies (at which the activity increased by 8% and 12%, respectively), while the action of the field of other frequencies studied (2; 5; 10; 30; 40 and 50 Hz) were found to deactivate the enzyme. Emamdadi et al. [42] observed a very significant enhancement in

the enzymatic activity of HRP against pyrogallol after its 30 min incubation in a 52 mT static magnetic field. Regarding radio frequency electromagnetic fields, Fortune et al. [45] have observed no nonthermal effect on HRP after the action of either a 13.56 MHz, 915 MHz or 2.45 GHz frequency. Of note, Yao et al. [46] have recently reported very interesting results regarding the activation of HRP by its radio frequency (27.12 MHz) heating at 50 °C.

Our present research is aimed at studying the indirect effect of glycerol flow through a cylindrical coil heat exchanger on HRP. With this purpose, we have employed the well-established approach based on AFM and spectrophotometry [15,17,28] for studying the effect of glycerol flow in a shielded coil on HRP. While AFM has allowed us to reveal an increase in the aggregation of HRP on the surface of mica substrates, an increase in its enzymatic activity against its substrate 2,2′-azino-bis(3-ethylbenzothiazoline-6-sulfonate) (ABTS) in solution has also been observed.

The data reported can be of interest for scientists studying the interaction of biological macromolecules with electromagnetic fields. It is to be emphasized that HRP has found numerous applications in biotechnology as a catalyst [49], and in diagnostics as a reporter enzyme [50]. Accordingly, our results can also find application in the development of water purification systems [51,52], food treatment methods [46] and biomarker detection systems [53], considering the development of enzyme-based biosensors [53] and bioreactors with surface-immobilized enzymes [52].

2. Materials and Methods

2.1. Chemicals and Protein

HRP enzyme (peroxidase from horseradish; Cat. #6782) and its substrate 2,2′-azino-bis(3-ethylbenzothiazoline-6-sulfonate) (ABTS) were purchased from Sigma. Disodium hydrogen orthophosphate, citric acid and hydrogen peroxide were purchased from Reakhim (Moscow, Russia). An amount of 2 mM Dulbecco's modified phosphate-buffered saline (PBSD buffer) was prepared from a salt mixture purchased from Pierce (Waltham, MA, USA). Ultrapure deionized water (with 18.2 MΩ × cm resistivity) was used in all the experiments. The water was purified using a Simplicity UV system (Millipore, Molsheim, France). Glycerol was purchased from Glaconchemie GmbH (Merseburg, Germany).

2.2. Experimental Setup

Experimental setup used in our present research was analogous to that described in detail in our previous papers [16,17]. The difference was that the coil was covered with ground-shielded aluminum foil in order to provide proper shielding of transverse electromagnetic radiation. The schematic drawing of the experimental setup is presented in Figure S1. The coil is schematically shown in Figure 1, and Figure S2 displays its photographic image.

In brief, glycerol was continuously pumped through a polymeric (silicone) coiled pipe at a flowrate of 9 L/s. The fluid was warmed up to 65 °C in order to provide enough fluidity, making its pumping possible at a desired flowrate. The entire pipe (both the coiled and the linear sections) was additionally covered with a heat insulator to prevent undesired heating of the enzyme samples, since heating can affect the enzyme properties [46,47]. In this way, the temperature of the enzyme samples was kept at 25 °C.

In our reported experiments, the working enzyme solution was placed at a 2 cm distance from the coil's side, while the control enzyme sample was placed three meters away from the coil. The distance between the coil and the working enzyme solution (2 cm) was approximately two times greater than the diameter of the test tube. This was the shortest distance from the coil, at which we could avoid direct physical contact between the test tube and the coil. The control sample was placed at the longest available distance from the coil. This distance in control experiments was limited by the size of the laboratory room and was 150 times greater than that in working experiments. The enzyme concentration of both the working and the control solution was 0.1 μM in 2 mM PBSD buffer (pH 7.4), and the volume of each sample solution was 1 mL. The enzyme solutions were incubated in

the designated locations for 40 min. After the incubation, the solutions were subjected to parallel AFM and spectrophotometric analysis.

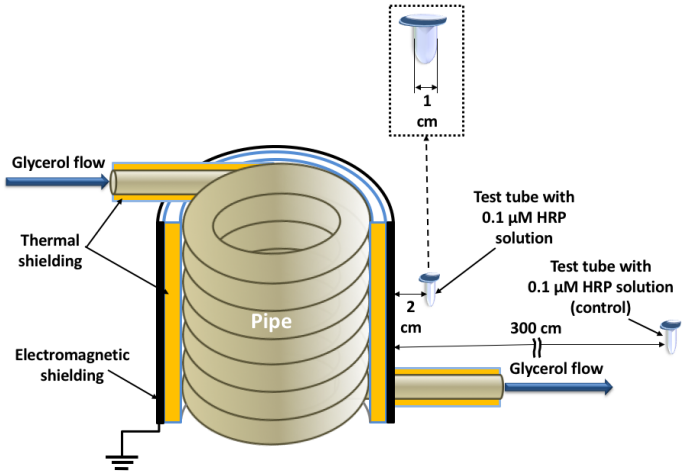

Figure 1. Experimental setup's key unit. The inset shows an enlarged picture of the ~1-cm diameter test tube. Thin lines indicate the distances between the coil and the test tubes with working and control HRP solutions.

2.3. AFM Experiments—Preparation of Substrates for AFM

Samples for AFM measurements were prepared by direct surface adsorption [54] as described in our previous papers [15–17,28]. In brief, one 7 mm × 15 mm piece of freshly cleaved muscovite mica (AFM substrate; Structure Probe, Inc., West Chester, PA, USA) was immersed into the test tube with the HRP sample to be studied, and kept therein for ten minutes upon shaking at 600 rpm and at room temperature. Then, the substrate was rinsed with ultrapure water and air-dried.

Blank experiments were performed with the use of pure enzyme-free buffer instead of HRP solution.

2.4. AFM Experiments—AFM Scanning

The mica AFM substrates with surface-adsorbed HRP particles were scanned with a Titanium atomic force microscope (NT-MDT, Zelenograd, Russia; the microscope pertains to the equipment of "Human Proteome" Core Facility of the Institute of Biomedical Chemistry, supported by Ministry of Education and Science of Russian Federation, agreement no. 14.621.21.0017, unique project ID: RFMEFI62117X0017). NSG10 AFM probes ("TipsNano", Zelenograd, Russia) with tip curvature radius of 10 nm (resonant frequency: 47 to 150 kHz; force constant: 0.35 to 6.1 N/m) were employed for AFM scanning. At least ten scans were obtained for each AFM substrate studied. Regarding the blank experiments, no objects with heights exceeding 0.5 nm were observed.

Microscope operation, treatment of the AFM images obtained (flattening correction, etc.) and exporting the AFM data to ASCII format were performed using a NOVA Px software (NT-MDT, Moscow, Zelenograd, Russia) supplied with the microscope. The number of the visualized particles in the obtained AFM images was calculated with a specialized AFM data processing software developed in IBMC.

The relative distribution of the AFM-visualized objects with height $\rho(h)$ (density function), and the number of particles visualized by AFM (normalized per 400 μm^2) were calculated for each sample studied as described by Pleshakova et al. [55].

Namely, $\rho(h)$ was calculated as follows:

$$\rho(h) = (N_h/N) \times 100\%, \quad (1)$$

where N_h is the number of distinct particles, imaged by AFM, with height h; and N is the total number of imaged distinct particles [55].

The number of particles N_{400}, normalized per 400 μm^2 area of the substrate surface, was calculated as:

$$N_{400} = N \times 400/(n \times d^2), \quad (2)$$

where N is the number of visualized objects for one and the same sample; n is the number of AFM scans performed for one and the same sample; and d is the linear dimension of the AFM scan (μm).

2.5. Spectrophotometric Determination of HRP Enzymatic Activity

Spectrophotometry measurements were performed according to a well-established technique described previously [15,17,28]; this technique, based on the interaction of the HRP enzyme with its substrate ABTS in slightly acidic (pH 5.0, as recommended by the enzyme manufacturer [56]) phosphate-citrate buffer, was originally reported by Sanders et al. [57]. When ABTS was used as HRP substrate, the use of phosphate-citrate buffer was reported to be a good practice [58]. The spectrophotometry measurements were carried out with an Agilent 8453 spectrophotometer (Agilent Deutschland GmbH, Waldbronn, Germany) at 405 nm. The absorbance A_{405} of phosphate-citrate buffer containing 1 nM HRP, 0.3 mM ABTS and 2.5 mM H_2O_2, was measured at 405 nm during the time t = 5 min. The results were presented in the form of $A_{405}(t)$ curves. The enzymatic activity was calculated based on the first 200 s of measurement as described previously [59].

3. Results

3.1. Atomic Force Microscopy

Figure 2 displays typical AFM images of HRP adsorbed onto mica from the control enzyme solution (which was incubated three meters away from the coil; Figure 2a) and from the working enzyme solution (which was incubated at a 2 cm distance from the coil's side; Figure 2b).

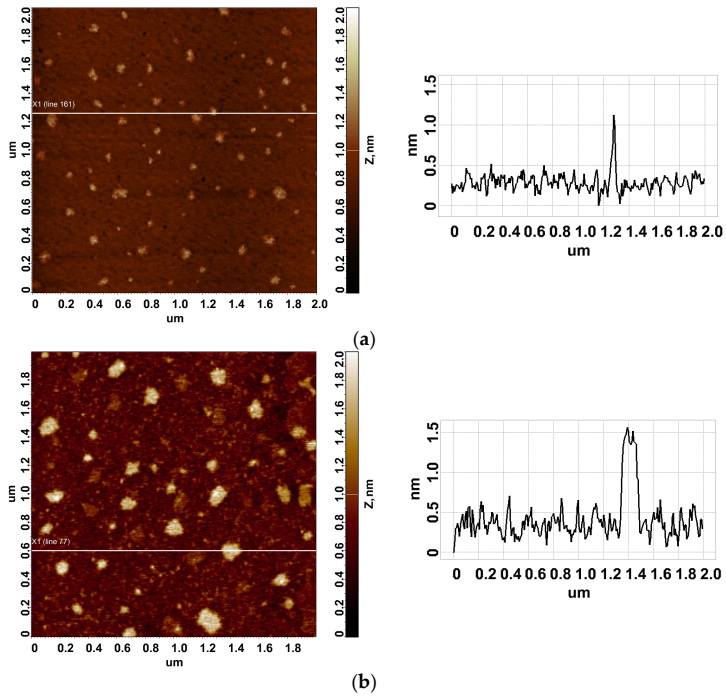

Figure 2. Typical AFM images of HRP adsorbed onto mica obtained in the case of control enzyme solution incubated three meters away from the coil (**a**) and in the case of working enzyme solution incubated at a 2 cm distance from the coil's side (**b**). Panels on the right display cross-section profiles corresponding to the lines in the respective AFM images on the left.

The representative images in Figure 2 indicate that HRP is adsorbed on mica in the form of compact objects. The results of processing the entire AFM data allowed us to determine whether there was an effect on HRP aggregation in our experiments.

Figure 3 displays $\rho(h)$ plots obtained for working (red curve) and control (blue curve) enzyme samples.

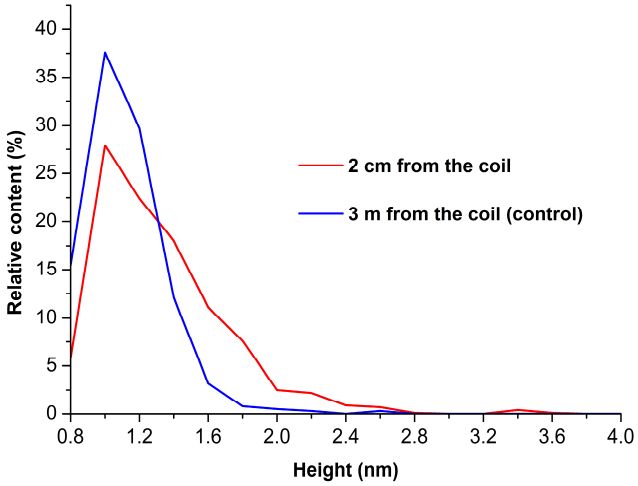

Figure 3. Density function $\rho(h)$ plots obtained for working HRP sample (incubated at a 2 cm distance from the coil's side; red curve) and for control HRP sample (incubated three meters away from the experimental setup; blue curve).

By analyzing the shape of the density functions' plots, one can observe an increase in the content of high (>1.4 nm) objects in the working enzyme sample in comparison with the control one. As justified previously [28], these high objects can be attributed to an aggregated form of mica-adsorbed HRP. Accordingly, this allows us to make a conclusion that the incubation of 0.1 μM HRP solution near the side of a shielded coil with flowing glycerol induces an aggregation of the enzyme upon its adsorption onto mica.

Figure 4 displays the absolute distribution of the number of particles, visualized by AFM on mica substrates, with height.

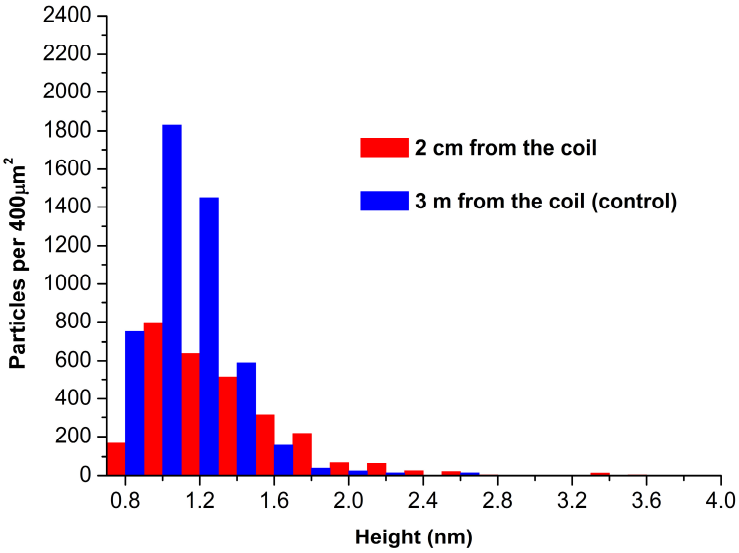

Figure 4. Number of AFM-visualized particles, normalized per 400 μm^2, obtained for a working HRP sample (incubated at a 2 cm distance from the coil's side; red bars) and for control HRP sample (incubated three meters away from the experimental setup; blue bars).

The data presented in Figure 4 indicate that the number of particles adsorbed from the working enzyme sample (red bars; N_{400} = 2800 particles per 400 μm^2) and that of particles adsorbed from the control enzyme sample (blue bars; N_{400} = 4800 particles per 400 μm^2) are of the same order of magnitude.

3.2. Spectrophotometric Determination of HRP Enzymatic Activity

Figure 5 displays $A_{405}(t)$ curves recorded at 405 nm for working (red curve) and control (blue curve) enzyme samples.

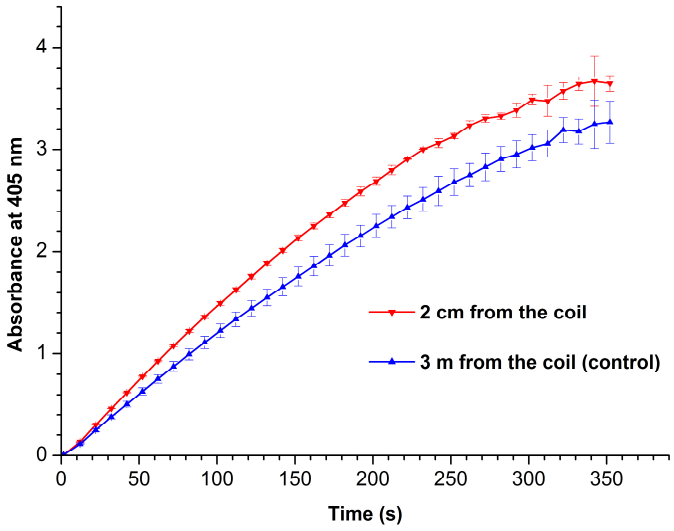

Figure 5. Absorbance at 405 nm vs. time curves recorded for a working HRP sample (incubated at a 2 cm distance from the coil's side; red curve) and for control HRP sample (incubated three meters away from the experimental setup; blue curve).

From Figure 5, one can see that the enzymatic activity of HRP after its incubation near the coil with flowing glycerol is considerably higher than that of the enzyme in the control sample. Indeed, the activity of the enzyme in the control sample was only 184 units/(mL enzyme), while that in the sample incubated near the coil's side was 222 units/(mL enzyme), i.e., 20% higher. This is in contrast to the previously reported case [17], in which the incubation of HRP near the outlet of the coil led to a 18% drop in its activity against ABTS. The phenomenon of considerable (by up to ~14%) enhancement of HRP enzymatic activity by external electromagnetic field has been previously observed by Yao et al. [46] after a radio frequency (27.12 MHz) treatment of this enzyme at high power (6 kW) and 50 °C. These authors also emphasized that a deactivation of the enzyme was observed at higher (70 °C and 90 °C) temperatures. This is why we have performed our best to provide proper heat insulation for the coil.

4. Discussion

In our present research, we have studied the influence of glycerol flow, organized in a ground-shielded cylindrical coil, on the properties of horseradish peroxidase enzyme. The adsorption properties of the enzyme have been investigated by AFM, while its enzymatic activity against ABTS substrate has been assessed by spectrophotometry.

Previously, in [60], it was noted that both moving and static objects can influence the aggregation state of enzymes. This phenomenon is called the "Ivanov–Tatur effect" [60]. Particularly, the case with an enzyme incubated above a coil with flowing glycerol [16] was emphasized [60].

According to our results, AFM has allowed us to reveal an increase in the HRP aggregation on mica. Moreover, a slight increase in the enzymatic activity of HRP has been observed after the incubation of the enzyme near the coil. These effects can be explained

by the action of an electromagnetic field, which is induced by the flow of glycerol, on the enzyme. The origin of this field can be explained by the occurrence of the so-called triboelectric effect. Below, we consider this phenomenon in more detail.

In our experimental setup, the flow of glycerol through a polymeric pipe has been organized. The flow of a liquid is known to be accompanied by friction between the liquid and the pipe surface [61]. And this friction is known to be the driving force of the triboelectric effect, which is also known as "friction-driven contact electrification" [62]. In general, this effect occurs in solid–solid [62,63], liquid–solid [10–21], solid–gas [64] and liquid–liquid [65] systems [62]. The motion of the triboelectrically generated charges induces an electromagnetic field. The exact fundamental origin of the triboelectric generation of charge was only recently explained from the viewpoint of thermoelectric physics [62]. Frictional heat was found to be a fundamental factor characterizing triboelectrification [62,63]. Shin et al. have explained the occurrence of a stronger triboelectric effect in insulating polymeric systems by the combination of their properties, namely their low density and thermal conductivity [62].

Based on the above information, the dielectric characteristics of the materials involved in the triboelectric system represent one of the factors influencing the triboelectric effect. Namely, stronger triboelectric effects were reported for the systems based on dielectric materials, in contrast to weaker ones observed for conducting systems [62,66]. Additionally, in this connection, we must emphasize that in our reported experiments, both the liquid (glycerol) and the solid (silicone pipe) are dielectrics, thus favoring the occurrence of a strong triboelectric effect.

Another important factor is the chemical composition of the triboelectric system materials. With regard to the liquid–solid systems, the triboelectric effect was reported to be dependent on the content of chemical groups in the liquid—apart from the dielectric properties of the materials involved [21]. Namely, in their very recent work, Yoo et al. found that in liquid–solid systems, hydroxyl groups enhance the triboelectric effect, while hydrocarbon groups suppress it [21]. Among the liquids studied by these authors, the strongest effect was observed for 70% sorbitol solution and glycerol (though the sorbitol solution contained water). It is to be noted that pure hydrocarbons (such as hexane) were not studied [21]. Nevertheless, the results reported by Yoo et al. revealed one more factor explaining strong triboelectric effects observed with glycerol.

It is to be emphasized that in our experiments reported herein, the coil with flowing glycerol has been ground-shielded. Thus, the effect observed in our experiments cannot be attributed to the action of a transverse electromagnetic radiation, which could take place if the coil was not ground-shielded. The phenomena revealed in our experiments can be explained by the formation of a longitudinal field by the flow of glycerol. The effect of such a field, intentionally formed by means of a specialized generator, on the enzyme was observed for the first time by Ivanov et al. [28]. It was noted that such electromagnetic fields, which have a specific topology [67–70], can influence biological objects (including enzymes) at even very low power densities, comparable with the background radiation level [22]. The effect of the field on both the enzyme aggregation and its enzymatic activity can be explained by the change in the structure of the enzyme's hydration shell under the action of the field.

Indeed, the structure of the hydration shell was shown to be one of the factors influencing the functioning of biological macromolecules [71]. And in the case of enzymes, their enzymatic activity can be well-affected by alterations in their hydration shells [71–73], and this is what we have observed in our experiments with HRP enzyme. This is how we explain the effect of glycerol flow on HRP enzyme in our particular case.

HRP is known to readily form aggregates, particularly at micromolar concentrations [74]. Considering the temperature range from 15 to 40 °C, the content of aggregates in the case of the adsorption of HRP on mica was found to be slightly higher at room temperature and pH 7.4 [75]. Here, it should be emphasized that the aggregation of an enzyme does not imply the loss of its activity. Although aggregated enzymes are often considered as less

active than non-aggregated ones [76], the existence of a correlation between the enzyme aggregation and enzymatic activity depends on the enzyme type. According to Gentile et al., no aggregation-induced attenuation of catalytic activity was revealed for hexokinase and alkaline phosphatase [77]. And in our experiments, we have observed an increase in the aggregation of HRP on mica accompanied by a 20% increase in its activity against ABTS.

The structural stability of HRP is known to be dependent on such important factors as temperature and pH [78]. The highest temperature stability of this enzyme was observed at pH > 6.5. In order to avoid an interference of the pH on the enzyme structure, prior to the incubation in the experimental setup, we had dissolved the enzyme in PBSD buffer with pH 7.4. Generally, both the high temperature and the acidic pH are known to be the factors inducing protein denaturation—that is, the partial or complete disarrangement of its spatial structure. The considerable unfolding of HRP tertiary and secondary structures was observed at acidic pH < 4.5 [78]. It is to be noted that pH directly influences the electrostatic mechanism of enzyme adsorption [79]. In general, enzyme adsorption represents a complex process, which involves the interactions of enzyme macromolecules with each other (that is, enzyme aggregation), with the surface and with the solvent [80]. Based on these considerations, we have conducted our experiments at room temperature and pH 7.4 in order to confirm that the observed effects on the enzyme aggregation and activity are only caused by the field generated in the experimental setup. The enzyme may behave differently upon a change in either the pH, the ionic strength or the temperature [79], and this should be studied in the future.

5. Conclusions

The flow of a dielectric liquid (glycerol) through a ground-shielded cylindrical coil has been found to affect the physicochemical properties of horseradish peroxidase enzyme, whose 0.1 μM solution has been incubated at a 2 cm distance from the coil for 40 min. Namely, such an incubation has led to an increased aggregation of the enzyme on mica, as has been revealed at the single-molecule level by atomic force microscopy. Moreover, its enzymatic activity against 2,2′-azino-bis(3-ethylbenzothiazoline-6-sulfonate) has been found to increase after the incubation near the coil—as compared with the control enzyme sample incubated three meters away from the coil. The results obtained can be of use in the development of triboelectric generators, and should be taken into consideration in the development of novel flow-based biosensors and bioreactors with surface-immobilized enzymes.

Supplementary Materials: The following supporting information can be downloaded at: https://www.mdpi.com/article/10.3390/app13137516/s1, Figure S1: Schematic drawing of the experimental setup; Figure S2: Photographic image of the shielded coil.

Author Contributions: Conceptualization, Y.D.I. and V.Y.T.; data curation, A.A.V., M.O.E., I.D.S. and A.F.K.; formal analysis, I.D.S., N.D.I. and V.S.Z.; investigation, Y.D.I., I.D.S., A.A.V., I.A.I., M.O.E. and V.S.Z.; methodology, Y.D.I. and V.Y.T.; project administration, Y.D.I.; resources, V.Y.T., A.A.L. and V.S.Z.; software, A.A.L.; supervision, Y.D.I.; validation, V.S.Z.; visualization, I.D.S., A.F.K. and A.A.V.; writing—original draft, I.D.S. and Y.D.I.; writing—review and editing, Y.D.I. All authors have read and agreed to the published version of the manuscript.

Funding: This work was financed by the Ministry of Science and Higher Education of the Russian Federation within the framework of state support for the creation and development of World-Class Research Centers 'Digital Biodesign and Personalized Healthcare' (No 075-15-2022-305).

Data Availability Statement: Correspondence and requests for materials should be addressed to Y.D.I.

Acknowledgments: The AFM measurements were performed employing a Titanium multimode atomic force microscope, which pertains to "Avogadro" large-scale research facilities.

Conflicts of Interest: The authors declare no conflict of interest.

References

1. Zhang, T.; Liu, C.; Gu, Y.; Jérôme, F. Glycerol in Energy Transportation: A State-of-the-art Review. *Green Chem.* **2021**, *23*, 7865–7889. [CrossRef]
2. Jacobsen, D.; McMartin, K.E. Alcohols and glycols. In *Human Toxicology*; Descotes, J., Ed.; Elsevier Science B.V.: Amsterdam, The Netherlands, 1996; pp. 623–648. [CrossRef]
3. Vijayendran, R.A.; Ligler, F.S.; Leckband, D.E. A computational reaction-diffusion model for the analysis of transport-limited kinetics. *Anal. Chem.* **1998**, *71*, 5405–5412. [CrossRef]
4. Teeparuksapun, K.; Hedström, M.; Mattiasson, B. A Sensitive Capacitive Biosensor for Protein a Detection Using Human IgG Immobilized on an Electrode Using Layer-by-Layer Applied Gold Nanoparticles. *Sensors* **2022**, *22*, 99. [CrossRef] [PubMed]
5. Kamat, V.; Rafique, A. Exploring sensitivity & throughput of a parallel flow SPRi biosensor for characterization of antibody-antigen interaction. *Anal. Biochem.* **2017**, *525*, 8–22. [CrossRef]
6. Yang, D.; Singh, A.; Wu, H.; Kroe-Barrett, R. Comparison of biosensor platforms in the evaluation of high affinity antibody-antigen binding kinetics. *Anal. Biochem.* **2016**, *508*, 78–96. [CrossRef]
7. Zhao, H.; Gorshkova, I.I.; Fu, G.L.; Schuck, P. A comparison of binding surfaces for SPR biosensing using an antibody–antigen system and affinity distribution analysis. *Methods* **2013**, *59*, 328–335. [CrossRef]
8. Dobson, J.; Kumar, A.; Willis, L.F.; Tuma, R.; Higazi, D.R.; Turner, R.; Lowe, D.C.; Ashcroft, A.E.; Radford, S.E.; Kapur, N.; et al. Inducing protein aggregation by extensional flow. *Proc. Natl. Acad. Sci. USA* **2017**, *114*, 4673–4678. [CrossRef]
9. Ravelo, B.; Duval, F.; Kane, S.; Nsom, B. Demonstration of the triboelectricity effect by the flow of liquid water in the insulating pipe. *J. Electrost.* **2011**, *69*, 473–478. [CrossRef]
10. Choi, D.; Lee, H.; Im, D.J.; Kang, I.S.; Lim, G.; Kim, D.S.; Kang, K.H. Spontaneous electrical charging of droplets by conventional pipetting. *Sci. Rep.* **2013**, *3*, 2037. [CrossRef]
11. Cheedarala, R.K.; Song, J.I. Harvesting of flow current through implanted hydrophobic PTFE surface within silicone-pipe as liquid nanogenerator. *Sci. Rep.* **2022**, *12*, 3700. [CrossRef]
12. Xu, W.; Zheng, H.; Liu, Y.; Zhou, X.; Zhang, C.; Song, Y.; Deng, X.; Leung, M.; Yang, Z.; Xu, R.X.; et al. A droplet-based electricity generator with high instantaneous power density. *Nature* **2020**, *578*, 392–396. [CrossRef]
13. Zhao, L.; Liu, L.; Yang, X.; Hong, H.; Yang, Q.; Wang, J.; Tang, Q. Cumulative charging behavior of water droplets driven freestanding triboelectric nanogenerator toward hydrodynamic energy harvesting. *J. Mater. Chem. A* **2020**, *8*, 7880–7888. [CrossRef]
14. Haque, R.I.; Arafat, A.; Briand, D. Triboelectric effect to harness fluid flow energy. *J. Phys. Conf. Ser.* **2019**, *1407*, 012084. [CrossRef]
15. Ivanov, Y.D.; Pleshakova, T.O.; Shumov, I.D.; Kozlov, A.F.; Romanova, T.S.; Valueva, A.A.; Tatur, V.Y.; Stepanov, I.N.; Ziborov, V.S. Investigation of the Influence of Liquid Motion in a Flow-based System on an Enzyme Aggregation State with an Atomic Force Microscopy Sensor: The Effect of Water Flow. *Appl. Sci.* **2020**, *10*, 4560. [CrossRef]
16. Ziborov, V.S.; Pleshakova, T.O.; Shumov, I.D.; Kozlov, A.F.; Ivanova, I.A.; Valueva, A.A.; Tatur, V.Y.; Negodailov, A.N.; Lukyanitsa, A.A.; Ivanov, Y.D. Investigation of the Influence of Liquid Motion in a Flow-Based System on an Enzyme Aggregation State with an Atomic Force Microscopy Sensor: The Effect of Glycerol Flow. *Appl. Sci.* **2020**, *10*, 4825. [CrossRef]
17. Ivanov, Y.D.; Pleshakova, T.O.; Shumov, I.D.; Kozlov, A.F.; Ivanova, I.A.; Ershova, M.O.; Tatur, V.Y.; Ziborov, V.S. AFM Study of the Influence of Glycerol Flow on Horseradish Peroxidase near the in/out Linear Sections of a Coil. *Appl. Sci.* **2021**, *11*, 1723. [CrossRef]
18. Xiao, S.; Wu, H.; Li, N.; Tan, X.; Deng, H.; Zhang, X.; Tang, J.; Li, Y. Triboelectric Mechanism of Oil-Solid Interface Adopted for Self-Powered Insulating Oil Condition Monitoring. *Adv. Sci.* **2023**, *10*, 2207230. [CrossRef]
19. Tanasescu, F.; Cramariuc, R. *Electrostatica în Technica*; Editura Technica: Bucharest, Romania, 1977.
20. Balmer, R. Electrostatic Generation in Dielectric Fluids: The Viscoelectric Effect. In Proceedings of the WTC2005 World Tribology Congress III, Washington, DC, USA, 12–16 September 2005. Paper No. WTC2005-63806. [CrossRef]
21. Yoo, D.; Jang, S.; Cho, S.; Choi, D.; Kim, D.S. A Liquid Triboelectric Series. *Adv. Mater.* **2023**, 2300699. [CrossRef]
22. Kushchev, L.A.; Okuneva, G.L.; Suslov, D.Y.; Gravin, A.A. Modeling biogas production in bubbling bioreactors. *Chem. Petrol. Eng.* **2012**, *47*, 613–618. [CrossRef]
23. Steudler, S.; Werner, A.; Cheng, J.J. (Eds.) *Solid State Fermentation. Research and Industrial Applications*; Springer Nature: Cham, Switzerland, 2019. [CrossRef]
24. Pino, M.S.; Rodríguez-Jasso, R.M.; Michelin, M.; Flores-Gallegos, A.C.; Morales-Rodriguez, R.; Teixeira, J.A.; Ruiz, H.A. Bioreactor design for enzymatic hydrolysis of biomass under the biorefinery concept. *Chem. Eng. J.* **2018**, *347*, 119–136. [CrossRef]
25. Ruggeri, F.S.; Šneideris, T.; Vendruscolo, M.; Knowles, T.P.J. Atomic force microscopy for single molecule characterisation of protein aggregation. *Arch. Biochem. Biophys.* **2019**, *664*, 134–148. [CrossRef]
26. Cawood, E.E.; Karamanos, T.K.; Wilson, A.J.; Radford, S.E. Visualizing and trapping transient oligomers in amyloid assembly pathways. *Biophys. Chem.* **2021**, *268*, 106505. [CrossRef]
27. Yang, H.; Wang, Y.; Lai, S.; An, H.; Li, Y.; Chen, F. Application of Atomic Force Microscopy as a Nanotechnology Tool in Food Science. *J. Food Sci.* **2007**, *72*, R65–R75. [CrossRef]
28. Ivanov, Y.D.; Pleshakova, T.O.; Shumov, I.D.; Kozlov, A.F.; Ivanova, I.A.; Valueva, A.A.; Tatur, V.Y.; Smelov, M.V.; Ivanova, N.D.; Ziborov, V.S. AFM imaging of protein aggregation in studying the impact of knotted electromagnetic field on a peroxidase. *Sci. Rep.* **2020**, *10*, 9022. [CrossRef]

29. Ivanov, Y.D.; Tatur, V.Y.; Pleshakova, T.O.; Shumov, I.D.; Kozlov, A.F.; Valueva, A.A.; Ivanova, I.A.; Ershova, M.O.; Ivanova, N.D.; Repnikov, V.V.; et al. Effect of Spherical Elements of Biosensors and Bioreactors on the Physicochemical Properties of a Peroxidase Protein. *Polymers* **2021**, *13*, 1601. [CrossRef]
30. Ivanov, Y.D.; Frantsuzov, P.A.; Zöllner, A.; Medvedeva, N.V.; Archakov, A.I.; Reinle, W.; Bernhardt, R. Atomic Force Microscopy Study of Protein–Protein Interactions in the Cytochrome CYP11A1 (P450scc)-Containing Steroid Hydroxylase System. *Nanoscale Res. Lett.* **2011**, *6*, 54. [CrossRef]
31. Ivanov, Y.D.; Bukharina, N.S.; Frantsuzov, P.A.; Pleshakova, T.O.; Kanashenko, S.L.; Medvedeva, N.V.; Argentova, V.V.; Zgoda, V.G.; Munro, A.W.; Archakov, A.I. AFM study of cytochrome CYP102A1 oligomeric state. *Soft Matter* **2012**, *8*, 4602–4608. [CrossRef]
32. Baron, A.M.; Lubambo, A.F.; Lima, V.M.G.; de Camargo, P.C.; Mitchell, D.A.; Krieger, N. Atomic Force Microscopy: A Useful Tool for Evaluating Aggregation of Lipases. *Microsc. Microanal.* **2005**, *11* (Suppl. 3), 74–77. [CrossRef]
33. Blasi, L.; Longo, L.; Vasapollo, G.; Cingolani, R.; Rinaldi, R.; Rizzello, T.; Acierno, R.; Maffia, M. Characterization of glutamate dehydrogenase immobilization on silica surface by atomic force microscopy and kinetic analyses. *Enz. Microbial Technol.* **2005**, *36*, 818–823. [CrossRef]
34. Zhang, P.; Tan, W. Atomic force microscopy for the characterization of immobilized enzyme molecules on biosensor surfaces. *Fresenius J. Anal. Chem.* **2001**, *369*, 302–307. [CrossRef]
35. Neeli, R.; Girvan, H.M.; Lawrence, A.; Warren, M.J.; Leys, D.; Scrutton, N.S.; Munro, A.W. The dimeric form of flavocytochrome P450 BM3 is catalytically functional as a fatty acid hydroxylase. *FEBS Lett.* **2005**, *579*, 5582–5588. [CrossRef]
36. Davies, P.F.; Rennke, H.G.; Cotran, R.S. Influence of molecular charge upon the endocytosis and intracellular fate of peroxidase activity in cultured arterial endothelium. *J. Cell Sci.* **1981**, *49*, 69–86. [CrossRef]
37. Welinder, K.G. Amino acid sequence studies of horseradish peroxidase. amino and carboxyl termini, cyanogen bromide and tryptic fragments, the complete sequence, and some structural characteristics of horseradish peroxidase C. *Eur. J. Biochem.* **1979**, *96*, 483–502. [CrossRef]
38. Tams, J.W.; Welinder, K.G. Mild chemical deglycosylation of horseradish peroxidase yields a fully active, homogeneous enzyme. *Anal. Biochem.* **1995**, *228*, 48–55. [CrossRef]
39. Veitch, N.C. Horseradish peroxidase: A modern view of a classic enzyme. *Phytochemistry* **2004**, *65*, 249–259. [CrossRef]
40. Ohshima, T.; Tamura, T.; Sato, M. Influence of pulsed electric field on various enzyme activities. *J. Elstat.* **2007**, *65*, 156–161. [CrossRef]
41. Wasak, A.; Drozd, R.; Jankowiak, D.; Rakoczy, R. The influence of rotating magnetic field on bio-catalytic dye degradation using the horseradish peroxidase. *Biochem. Eng. J.* **2019**, *147*, 81–88. [CrossRef]
42. Emamdadi, N.; Gholizadeh, M.; Housaindokht, M.R. Investigation of static magnetic field effect on horseradish peroxidase enzyme activity and stability in enzymatic oxidation process. *Int. J. Biol. Macromol.* **2021**, *170*, 189–195. [CrossRef]
43. Sun, J.; Sun, F.; Xu, B.; Gu, N. The quasi-one-dimensional assembly of horseradish peroxidase molecules in presence of the alternating magnetic field. *Coll. Surf. A Physicochem. Eng. Aspects* **2010**, *360*, 94–98. [CrossRef]
44. Sun, J.; Zhou, H.; Jin, Y.; Wang, M.; Gu, N. Magnetically enhanced dielectrophoretic assembly of horseradish peroxidase molecules: Chaining and molecular monolayers. *Chem. Phys. Chem.* **2008**, *9*, 1847–1850. [CrossRef]
45. Fortune, J.A.; Wu, B.-I.; Klibanov, A.M. Radio Frequency Radiation Causes No Nonthermal Damage in Enzymes and Living Cells. *Biotechnol. Prog.* **2010**, *26*, 1772–1776. [CrossRef]
46. Yao, Y.; Zhang, B.; Pang, H.; Wang, Y.; Fu, H.; Chen, X.; Wang, Y. The effect of radio frequency heating on the inactivation and structure of horseradish peroxidase. *Food Chem.* **2023**, *398*, 133875. [CrossRef]
47. Lopes, L.C.; Barreto, M.T.; Gonçalves, K.M.; Alvarez, H.M.; Heredia, M.F.; De Souza, R.O.M.; Cordeiro, Y.; Dariva, C.; Fricks, A.T. Stability and structural changes of horseradish peroxidase: Microwave versus conventional heating treatment. *Enzym. Microb. Technol.* **2015**, *69*, 10–18. [CrossRef]
48. Caliga, R.; Maniu, C.L.; Mihăşan, M. ELF-EMF exposure decreases the peroxidase catalytic efficiency in vitro. *Open Life Sci.* **2016**, *11*, 71–77. [CrossRef]
49. Bilal, M.; Rasheed, T.; Zhao, Y.; Iqbal, H.M.N. Agarose-chitosan hydrogel-immobilized horseradish peroxidase with sustainable bio-catalytic and dye degradation properties. *Int. J. Biol. Macromol.* **2019**, *124*, 742–749. [CrossRef]
50. Krainer, F.W.; Glieder, A. An updated view on horseradish peroxidases: Recombinant production and biotechnological applications. *Appl. Microbiol. Biotechnol.* **2015**, *99*, 1611–1625. [CrossRef]
51. Maryskova, M.; Linhartova, L.; Novotny, V.; Rysova, M.; Cajthaml, T.; Sevcu, A. Laccase and horseradish peroxidase for green treatment of phenolic micropollutants in real drinking water and wastewater. *Environ. Sci. Pollut. Res.* **2021**, *28*, 31566–31574. [CrossRef]
52. Bayramoğlu, G.; Arıca, M.Y. Enzymatic removal of phenol and p-chlorophenol in enzyme reactor: Horseradish peroxidase immobilized on magnetic beads. *J. Hazard. Mater.* **2008**, *156*, 148–155. [CrossRef]
53. Zhao, Y.; Zheng, Y.; Kong, R.; Xia, L.; Qu, F. Ultrasensitive electrochemical immunosensor based on horseradish peroxidase (HRP)-loaded silica-poly(acrylic acid) brushes for protein biomarker detection. *Biosens. Bioelectron.* **2016**, *75*, 383–388. [CrossRef]
54. Kiselyova, O.I.; Yaminsky, I.; Ivanov, Y.D.; Kanaeva, I.P.; Kuznetsov, V.Y.; Archakov, A.I. AFM study of membrane proteins, cytochrome P450 2B4, and NADPH–Cytochrome P450 reductase and their complex formation. *Arch. Biochem. Biophys.* **1999**, *371*, 1–7. [CrossRef]

55. Pleshakova, T.O.; Kaysheva, A.L.; Shumov, I.D.; Ziborov, V.S.; Bayzyanova, J.M.; Konev, V.A.; Uchaikin, V.F.; Archakov, A.I.; Ivanov, Y.D. Detection of hepatitis C virus core protein in serum using aptamer-functionalized AFM chips. *Micromachines* **2019**, *10*, 129. [CrossRef]
56. Enzymatic Assay of Peroxidase (EC 1.11.1.7) 2,20-Azino-Bis(3-Ethylbenzthiazoline-6-Sulfonic Acid) as a Substrate Sigma Prod. No. P-6782. Available online: https://www.sigmaaldrich.com/RU/en/technical-documents/protocol/protein-biology/enzymeactivity-assays/enzymatic-assay-of-peroxidase-abts-as-substrate (accessed on 18 February 2022).
57. Sanders, S.A.; Bray, R.C.; Smith, A.T. pH-dependent properties of a mutant horseradish peroxidase isoenzyme C in which Arg38 has been replaced with lysine. *Eur. J. Biochem.* **1994**, *224*, 1029–1037. [CrossRef]
58. Drozd, M.; Pietrzak, M.; Parzuchowski, P.G.; Malinowska, E. Pitfalls and capabilities of various hydrogen donors in evaluation of peroxidase-like activity of gold nanoparticles. *Anal. Bioanal. Chem.* **2016**, *408*, 8505–8513. [CrossRef]
59. Ivanov, Y.D.; Tatur, V.Y.; Shumov, I.D.; Kozlov, A.F.; Valueva, A.A.; Ivanova, I.A.; Ershova, M.O.; Ivanova, N.D.; Stepanov, I.N.; Lukyanitsa, A.A.; et al. The Effect of a Dodecahedron-Shaped Structure on the Properties of an Enzyme. *J. Funct. Biomater.* **2022**, *13*, 166. [CrossRef]
60. Shipov, G.I. Changing the properties of biomolecules under the influence of the shape of objects and their movement. *Zametki Uchenogo (Sci. Notes)* **2021**, *9-1*, 66–69.
61. Pouplin, A.; Masbernat, O.; Décarre, S.; Liné, A. Wall friction and effective viscosity of a homogeneous dispersed liquid–liquid flow in a horizontal pipe. *AIChE J. Fluid Mech. Transp. Phenom.* **2011**, *57*, 1119–1131. [CrossRef]
62. Shin, E.-C.; Ko, J.-H.; Lyeo, H.-K.; Kim, Y.-H. Derivation of a governing rule in triboelectric charging and series from thermoelectricity. *Phys. Rev. Res.* **2022**, *4*, 023131. [CrossRef]
63. Lee, D.W.; Kong, D.S.; Kim, J.H.; Park, S.H.; Hu, Y.C.; Ko, Y.J.; Jeong, C.B.; Lee, S.; Choi, J.I.J.; Lee, G.-H.; et al. Correlation between frictional heat and triboelectric charge: In operando temperature measurement during metal-polymer physical contact. *Nano Energy* **2022**, *103 Pt A*, 107813. [CrossRef]
64. Ducati, T.R.; Simões, L.H.; Galembeck, F. Charge partitioning at gas-solid interfaces: Humidity causes electricity buildup on metals. *Langmuir* **2010**, *26*, 13763. [CrossRef]
65. Nie, J.; Wang, Z.; Ren, Z.; Li, S.; Chen, X.; Wang, Z.L. Power generation from the interaction of a liquid droplet and a liquid membrane. *Nat. Commun.* **2019**, *10*, 2264. [CrossRef]
66. Pan, S.; Zhang, Z. Fundamental theories and basic principles of triboelectric effect: A review. *Friction* **2019**, *7*, 2–17. [CrossRef]
67. Ranada, A.F. Knotted solutions of the Maxwell equations in vacuum. *J. Phys. A Math. Gen.* **1990**, *23*, L815. [CrossRef]
68. Lee, W.; Gheorghe, A.; Tiurev, K.; Ollikainen, T.; Möttönen, M.; Hall, D.S. Synthetic electromagnetic knot in a three-dimensional skyrmion. *Sci. Adv.* **2018**, *4*, eaao3820. [CrossRef]
69. Smelov, M.V. Experimental study of nodular antennas in the form of shamrock and pentacle. *Radio Eng.* **2013**, *2*, 023–029.
70. Nefedov, E.I.; Ermolaev, Y.M.; Smelov, M.V. Experimental study of excitation and propagation of nodular electromagnetic waves in various media. *Radio Eng.* **2014**, *2*, 31–34.
71. Fogarty, A.C.; Laage, D. Water Dynamics in Protein Hydration Shells: The Molecular Origins of the Dynamical Perturbation. *J. Phys. Chem. B* **2014**, *118*, 7715–7729. [CrossRef]
72. Verma, P.K.; Rakshit, S.; Mitra, R.K.; Pal, S.K. Role of hydration on the functionality of a proteolytic enzyme α-chymotrypsin under crowded environment. *Biochimie* **2011**, *93*, 1424–1433. [CrossRef]
73. Laage, D.; Elsaesser, T.; Hynes, J.T. Water Dynamics in the Hydration Shells of Biomolecules. *Chem. Rev.* **2017**, *117*, 10694–10725. [CrossRef]
74. Ignatenko, O.V.; Sjölander, A.; Hushpulian, D.M.; Kazakov, S.V.; Ouporov, I.V.; Chubar, T.A.; Poloznikov, A.A.; Ruzgas, T.; Tishkov, V.I.; Gorton, L.; et al. Electrochemistry of chemically trapped dimeric and monomeric recombinant horseradish peroxidase. *Adv. Biosens. Bioelectron.* **2013**, *2*, 25–34.
75. Ivanova, I.A.; Ershova, M.O.; Shumov, I.D.; Valueva, A.A.; Ivanov, Y.D.; Pleshakova, T.O. Atomic Force Microscopy Study of the Temperature and Storage Duration Dependencies of Horseradish Peroxidase Oligomeric State. *Biomedicines* **2022**, *10*, 2645. [CrossRef]
76. Schramm, F.D.; Schroeder, K.; Jonas, K. Protein aggregation in bacteria. *FEMS Microbiol. Rev.* **2020**, *44*, 54–72. [CrossRef]
77. Gentile, K.; Bhide, A.; Kauffman, J.; Ghosh, S.; Maiti, S.; Adair, J.; Lee, T.-H.; Sen, A. Enzyme aggregation and fragmentation induced by catalysis relevant species. *Phys. Chem. Chem. Phys.* **2021**, *23*, 20709–20717. [CrossRef]
78. Chattopadhyay, K.; Mazumdar, S. Structural and Conformational Stability of Horseradish Peroxidase: Effect of Temperature and pH. *Biochemistry* **2000**, *39*, 263–270. [CrossRef]
79. Andrade, J.D.; Hlady, V.; Wei, A.P. Adsorption of complex proteins at interfaces. *Pure Appl. Chem.* **1992**, *64*, 1777–1781. [CrossRef]
80. Ziborov, V.S.; Pleshakova, T.O.; Shumov, I.D.; Kozlov, A.F.; Valueva, A.A.; Ivanova, I.A.; Ershova, M.O.; Larionov, D.I.; Evdokimov, A.N.; Tatur, V.Y.; et al. The Impact of Fast-Rise-Time Electromagnetic Field and Pressure on the Aggregation of Peroxidase upon Its Adsorption onto Mica. *Appl. Sci.* **2021**, *11*, 11677. [CrossRef]